Applied Catalysis B: Environmental 188 (2016) 106–112

Contents lists available at ScienceDirect

Applied Catalysis B: Environmental

journal homepage: www.elsevier.com/locate/apcatb

Hydrogen peroxide and photocatalysis

K. Sahel[a,b], L. Elsellami[a,c], I. Mirali[b], F. Dappozze[a], M. Bouhent[b], C. Guillard[a,*]

[a] IRCELYON, CNRS, UMR 5256/Université de Lyon, 2 Av. Albert Einstein, Villeurbanne Cedex 69626, France
[b] Laboratoire des Eco-Matériaux Fonctionnels et Nanostructurés, Faculté de Chimie, Département Génie des Matériaux, Université des Sciences et de la Technologie d'Oran (USTO), Oran, Algeria
[c] Unité de Recherche Catalyse et Matériaux pour l'Environnement et les Procédés URCMEP (UR11ESB5), Campus Universitaire Hatem Bettahar-Cité Elrriadh, 6072 Gabes, Tunisia

ARTICLE INFO

Article history:
Received 26 October 2015
Received in revised form
17 December 2015
Accepted 28 December 2015
Available online 22 January 2016

Keywords:
Photocatalysis
TiO_2
Rutile
Anatase
H_2O_2

ABSTRACT

The formation, the adsorption and the degradation of H_2O_2 on different commercial TiO_2 samples (anatase, rutile) and on ZnO have been investigated to better understand its participation in the photocatalytic reactions.

The Langmuir and Langmuir–Hinshelwood models have been used for determining the adsorption constants and the rate constants of H_2O_2 disappearance on these different photocatalysts both in the dark and under UV-A irradiation.

Interaction between H_2O_2 and TiO_2 has been investigated by UV–vis spectroscopy.

The adsorption of H_2O_2 on TiO_2 samples is discussed in term of surface area and nature of TiO_2 including the number of OH groups present on the photocatalysts. The nature of the yellow complex formed between H_2O_2 and TiO_2 is discussed taking into account its stability, and the coverage rate of OH groups.

The kinetic of H_2O_2 disappearance on the different photocatalysts is related to the adsorption but also the energy of conduction band of anatase and rutile photocatalysts.

The results of the formation and decomposition of H_2O_2 under UV-A irradiation in the presence of ZnO photocatalyst are explained in light of its adsorption.

1. Introduction

TiO_2-based photocatalysis is considered as an efficient process to remove air or water pollutants and it is well established that O_2 is essential in the process. It is also well known that electrons and holes generated react with H_2O and O_2 to form Reactive Oxygen Species (ROS) such as $OH^\bullet$, $HO_2^\bullet$, $O_2^{\bullet-}$, H_2O_2. Among the various Reactive Oxygen Species present in the mechanism of photocatalysis, H_2O_2 is the most stable species. H_2O_2 can serve as a reservoir of active ROS. Actually, some papers show the formation of $O_2^{\bullet-}$, $HO_2^\bullet$ or $OH^\bullet$ depending of conditions and nature of catalyst [1–3] and one of our previous publication has also shown the participation of H_2O_2 in the photocatalytic degradation of organics [4].

H_2O_2 is a very simple molecule but its behavior on semiconductor is very complex. Actually, it can be formed but also decomposed during the photocatalytic process.

It can be formed either by reduction of oxygen to form superoxide radicals $O_2^{\bullet-}$ (Reaction (R1)) which are in equilibrium with hydro-peroxide radicals in presence of protons (Reaction (R2)) [5].

$$O_2 + e^- \rightarrow (O_2^{\bullet-})s \quad \text{(R1)}$$

$$(O_2^{\bullet-})s + H^+ \rightarrow (HO_2^\bullet)s \quad \text{(R2)}$$

These radicals can be further reduced by electrons (Reaction (R3)) and then form hydrogen peroxide (H_2O_2) (Reaction (R4)) [5].

$$(HO_2^\bullet)s + e^- \rightarrow (HO_2^-)s \quad \text{(R3)}$$

$$(HO_2^-)s + H^+ \rightarrow (H_2O_2)s \quad \text{(R4)}$$

Another potential route for formation of hydrogen peroxide is the oxidation of water by photo- generated holes, forming hydroxyl radicals (Reaction (R5)), which can dimerize at the surface of the photocatalyst (Reaction (R6)) [3]. Considering, the adsorption energy of the HO radicals onto the surface of TiO_2 ($\Delta E = -4$ eV) [6], this most likely makes their desorption and recombination a process with a positive ΔG at room temperature.

$$H_2O + h+ \rightarrow OH^\bullet + H^+ \quad \text{(R5)}$$

$$OH^\bullet + OH^\bullet \rightarrow H_2O_2 \quad \text{(R6)}$$

* Corresponding author. Fax: +33 4 72 44 53 99.
E-mail addresses: chantal.guillard@ircelyon.univ-lyon1.fr, chantal.guillard@univ-lyon1.fr (C. Guillard).

http://dx.doi.org/10.1016/j.apcatb.2015.12.044
0926-3373/

However, it is very difficult to observe and quantify H_2O_2 due to its rapid decomposition on TiO_2 catalysts either by reduction (Reaction (R7)) or oxidation (Reaction (R8)) [5–9]. However some publications mentioned H_2O_2 in the gas phase near TiO_2 surfaces [10]. Nosaka et al. succeeded in quantifying the amount of H_2O_2 during photocatalysis. They found a H_2O_2 concentration in the order of the nmol/L [11].

$$H_2O_2 + 2e^- + 2H^+ \rightarrow 2H_2O \quad \text{(R7)}$$

$$H_2O_2 + 2h^+ \rightarrow O_2 + 2H^+ \quad \text{(R8)}$$

Taking into account that H_2O_2 can serve as a reservoir of more active ROS and that the impact of these relatively stable ROS on the mechanism of photocatalysis is not clear, in this work we propose to investigate the impact of the surface area and of the nature of TiO_2 (anatase, and rutile) on the adsorption and the decomposition of H_2O_2 but also on the UV–vis absorption properties. The formation and decomposition of hydrogen peroxide on ZnO is also studied because of its similar band gap and the absence of adsorption of H_2O_2 on this semiconductor. A relation between adsorption, nature and disappearance rate will be discussed.

2. Experimental

2.1. Photocatalysts and H_2O_2

One commercial Zinc oxide from Sigma–Aldrich and seven commercial titanium dioxide were used: titania Degussa P-25 which is made of anatase (80%) and rutile (20%), a 100% rutile sample from ISK (Ishihara Sangyo Kaisha), Japan; five anatase structures: PC105 and PC500 titanium dioxide from Millennium, AN1 and AN2 from Nanostructured and Amorphous Materials Inc and Hombikat UV100 purchased from Sachtleben Chemie (Duisburg, Germany). The characterizations of these catalysts, given by the producer of these commercial catalysts, are introduced in Table 1. H_2O_2 at 50% in water from Sigma–Aldrich is used in our experiments.

2.2. Photoreactor and light source

Irradiation was performed in a 1 L cylindrical glass reactor. Irradiation was provided by a 125 W UV-lamp Philips HPK placed in a plunging tube. A Pyrex cylindrical jacket located around the plunging tube contained circulating water to absorb IR radiation and avoid heating of the solution. The irradiance is measured by a digital radiometer (VLX-3W, UVItec) and was of 4 mW/cm^2.

2.3. Experimental procedures

2.3.1. Adsorption

A volume of 750 mL of aqueous solution with various initial concentrations of H_2O_2 was stirred in the dark in presence of photocatalyst at a concentration equal to 0.5 g L^{-1}. Ultrapure water (18 MΩ cm^{-1}) from Millipore Waters Milli-Q purification unit was used for all experiments. The concentration of the catalyst (0.5 g/L) has been chosen for a full absorption of the incident photon flux. Samples were withdrawn at regular intervals, centrifuged and analysed in order to monitor the H_2O_2 concentration.

2.3.2. Photocatalytic procedure

Before irradiation, H_2O_2/photocatalysts mixtures were stirred in the dark until the adsorption equilibrium was reached. Then, samples were collected from the reactor at regular time intervals and filtered through 0.45 μm millipores Durapore discs to remove photocatalyst powder before analysis.

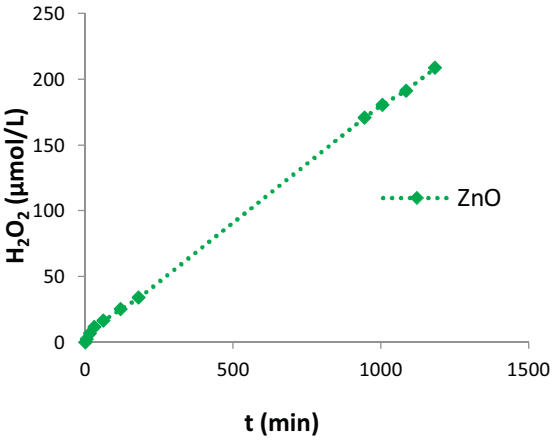

Fig. 1. Formation of H_2O_2 as a function of irradiation time in presence of 0.5 g/L of ZnO and water.

2.3.3. Analysis

H_2O_2 was complexed with an acidic solution of $TiCl_4$. Then, the H_2O_2 content of each sample was monitored at 410 nm by performing UV–vis spectroscopy in order to detect the yellow complex formed under acidic conditions in the presence of Ti^{4+} ions [12,13].

The UV–vis absorption spectra of complex formed between photocatalyst and H_2O_2 were recorded using a CCD Spectrometer Avantes AvaSpec-ULS2048. An optical fiber cable with a cosine corrector (CC-UV/VIS) enables punctual light emission measurements. The cosine corrector diameter is 3.9 mm for a measurement area of 12 mm^2.

3. Results and discussion

3.1. Formation of H_2O_2 on TiO_2 and on ZnO photocatalysts

Before studying the decomposition of H_2O_2 on illuminated various TiO_2 and on ZnO, we investigated the production of hydrogen peroxide and evaluated the impact of the surface area. H_2O_2 was detected only in the case of TiO_2 having a surface area higher than 200 m^2/g. However, the amounts are very low and correspond to less than 0.02 μmol/L. So, it seems that high surface areas favor the production of H_2O_2. Unfortunately, taking into account the very low concentration of H_2O_2 detected, these results do not allow us to clearly conclude on the impact of the surface and structure of TiO_2. In the presence of ZnO, a continuous formation of H_2O_2 was observed with a rate of about 0.18 μmol/L/min (Fig. 1).

The low concentration of H_2O_2 detected in presence of illuminated TiO_2 aqueous suspension, is in agreement with the literature [14,15]. For example, Nosaka et al. [11] reported the detection of H_2O_2 in concentrations as small as 10^{-9} M in presence of TiO_2. Boonstra et al. [16] suggested that the different behaviors of TiO_2 and ZnO can be explained by the absence of adsorption of H_2O_2 on zinc oxide. Our results given in Section 3.2.1 are in agreement with this hypothesis showing the necessity of interaction between photocatalyst surface and H_2O_2 to be degraded.

To better understand the pathways of production of hydrogen peroxide, hole scavengers have been used by different authors [5,17–19]. All these works reported that the presence of scavengers of holes on TiO_2 anatase improved the formation of H_2O_2. Moreover, Tafalla et al. [20] showed that an increasing in oxygen in the suspension improves the production of H_2O_2. These different works, performed on anatase TiO_2 samples, are in agreement with the production of H_2O_2 mainly by reduction of oxygen.

Table 1
Characterization of the various photocatalysts.

Photo-catalyst	P25	PC500	Hombikat UV100	TiO_2 NA1	TiO_2 NA2	PC105	Rutile	ZnO
Structure	80% Anatase 20% Rutile	Anatase	Anatase	Anatase	Anatase	Anatase	Rutile	
BET surface area (m^2/g)	50	340	330	240	200–220	88	103	11
Primary particle size (nm)	30	5–10	<10	15	10/30	15–25	13	50

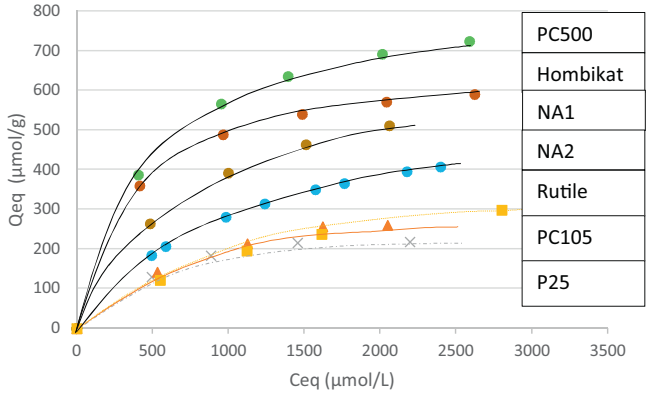

Fig. 2. Adsorption isotherm of H_2O_2 on different TiO_2 samples based on Reaction (R2).

3.2. Adsorption of H_2O_2 on different TiO_2 samples and on ZnO

3.2.1. Adsorption isotherm

Considering our results of H_2O_2 formation on different TiO_2 samples and on ZnO and since H_2O_2 is often mentioned as one of the intermediate species in TiO_2-based photocatalytic reactions [21], it is important to study the impact of the TiO_2 surface area and of the TiO_2 phase on the adsorption isotherm of H_2O_2 and to evaluate the equilibrium constants.

In order to ensure that the adsorption process reached equilibrium, different concentrations of H_2O_2 were stirred in the dark in the presence of TiO_2 and of ZnO and analysed as a function of time. In all cases, the H_2O_2 adsorption reached the equilibrium after about 60 min.

The amount of H_2O_2 adsorbed per gram of TiO_2 (Q_{eq}) is represented as a function of the equilibrium concentration (C_{eq}) in Fig. 2. In dark conditions, the amounts of H_2O_2 adsorbed on the TiO_2 surface (Q_{eq}) increase with the equilibrium concentration until reaching a plateau. In the presence of ZnO, no adsorption of H_2O_2 occurred. This result is in agreement with the work of Boonstra et al. [16] and can explain its formation and continuous evolution during irradiation of an aqueous suspension of ZnO.

The adsorption isotherm is in agreement with the Langmuir model. This model can be characterized as a monolayer adsorption on a homogeneous surface without interaction between adsorbed molecules. All adsorption sites are considered identical and the adsorbent has a maximum sorption capacity.

From Fig. 2, adsorption constants (K_{dark}) and the maximum amount of H_2O_2 (Q_{max}) adsorbed for each photocatalyst can be determined by the method of the least squares fitting according to the Eq. (1).

$$Q_{eq} = \frac{K_{dark} Q_{max} C_{eq}}{1 + K_{dark} C_{eq}} \quad (1)$$

where Q_{eq} is the adsorbed quantity of H_2O_2 and C_{eq} is the concentration of the compound at the adsorption equilibrium.

The values of the Langmuir parameters, Q_{max} and K_{dark}, are presented in Table 2.

We noticed that the more important the surface area, the larger the number of H_2O_2 moles adsorbed. Fig. 3a shows the correlation

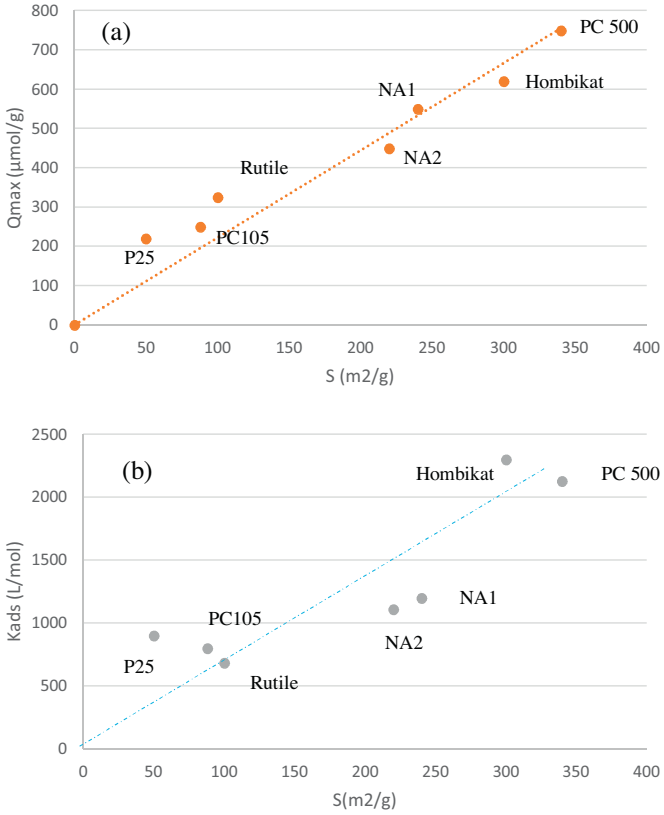

Fig. 3. Variation of Q_{max} (a) and K_{dark} (b) as a function of surface area of the catalyst.

between Q_{max} and the surface area of the catalysts. More surprisingly, a correlation was also observed between the surface and the adsorption constant (K_{dark}) (Fig. 3b) but it has not been yet explained.

Considering the surface area of these catalysts, we determined the number of H_2O_2 molecules adsorbed per nm^2 of TiO_2 (Table 2) and found that the number of H_2O_2 molecules adsorbed per nm^2 is about 1.2–1.5 molecules/nm^2 for NA1, NA2, Hombikat and PC500 and PC105 which are all pure anatase phase, whereas it is slightly more important for a pure rutile (1.9 molecules/nm^2) and much more important for P25 which is a mixture of anatase and rutile (2.7 molecules/nm^2).

These results indicate that for pure anatase phase, the amount of H_2O_2 molecules adsorbed vary linearly with their surface areas. The number of H_2O_2 molecules adsorbed per nm^2 of TiO_2 is in agreement with the value of 1.8 molecules/nm^2, found by Boonstra et al. [16] for a pure anatase phase of 110 m^2/g. However, the presence of rutile structure seems to improve the number of H_2O_2 adsorbed per nm^2. This behavior is mainly observed with TiO_2 P25. Actually, about two times more hydrogen peroxide moles are adsorbed per nm^2. In the case of pure rutile, only a slightly more important amount of H_2O_2 is adsorbed per nm^2 contrarily to the results obtained by Boonstra et al. [16] on rutile sample having similar surface area, one molecule of H_2O_2/nm^2 is adsorbed on rutile structure against 1.8 molecule of H_2O_2/nm^2 on anatase structure.

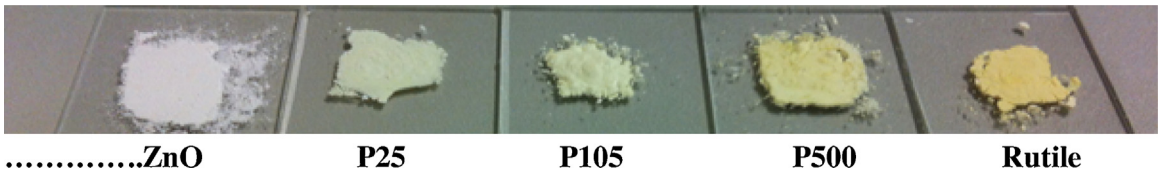

Fig. 4. Photos of various TiO_2 samples and of one ZnO sample in presence of H_2O_2.

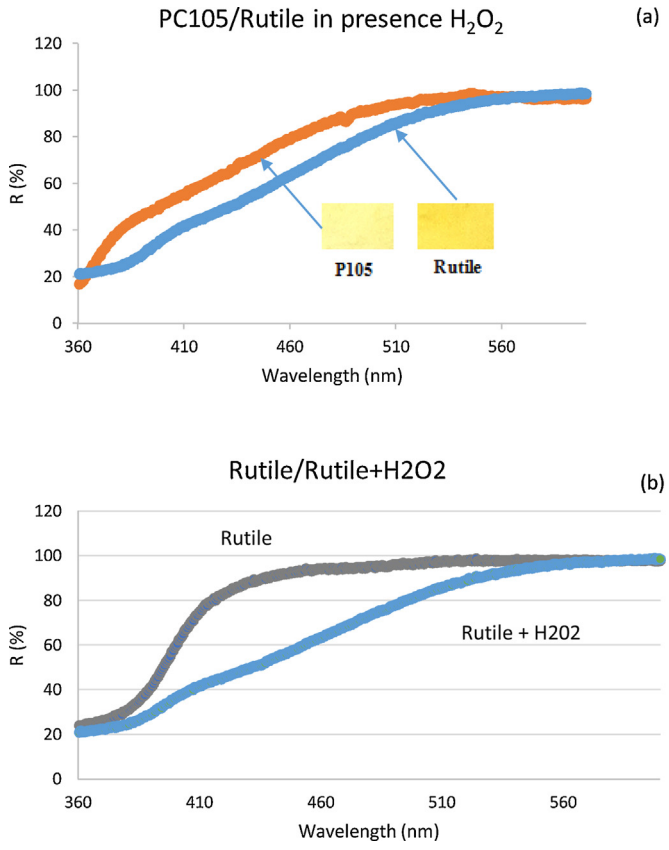

Fig. 5. (a) Reflectance spectra of PC105 (S = 88 m^2/g) and Rutile (S = 103 m^2/g) pretreated with H_2O_2 25%. (b) reflectance spectra of rutile and rutile/H_2O_2.

3.3. Interaction of H_2O_2 with TiO_2 surface in the dark

It is well known that when TiO_2 samples are suspended in an aqueous solution containing H_2O_2, a yellow complex appeared as already observed by different authors [16,22,23]. All TiO_2 samples, anatase, rutile and anatase/rutile phases became yellow-colored after adding 50 μL of a solution of 25% H_2O_2 on 100 mg of TiO_2. A stronger coloration was observed for samples with a larger specific surface area of TiO_2 (Fig. 4). This result is in agreement with Q_{max} obtained (Fig. 3a). On the rutile sample, the coloration is more important than that observed on anatase PC105 samples, which has a similar surface area confirming the higher number of H_2O_2 molecules adsorbed per nm^2. Coloration and reflectance spectra are given in Figs. 4 and 5.

It is also interesting to mention the high stability of these complexes during more than one day.

On anatase or rutile surfaces, there are valence-unfilled Ti(IV) ions centers and O(II) centers [24]. In the presence of H_2O_2, it is well know that a yellow complex corresponding to Ti-peroxo species is formed between Ti(IV) and H_2O_2 [25–27]. However, it is difficult to speculate on the species which are formed and on the exact surface structure that exists at the complex solid/solution interface. Three Ti-peroxo complexes are proposed, Ti-η^2-peroxide and two forms of Ti-μ-peroxide as given below:

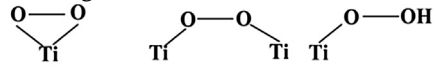

Ti-η^2-peroxide Ti-μ-peroxide

Ohno et al. [26] studied the nature of this complex by using Fourier Transform Infrared Spectroscopy, and X-ray photoelectron spectroscopy. They found that Ti-η^2-peroxide is the main Ti-peroxo complex formed on the surface of rutile TiO_2 whereas Ti-μ-peroxide is mainly generated on the anatase phase [26]. However a density functional theory study on the reactions of H_2O_2 on anatase and rutile TiO_2 surfaces indicates that for both phases, the more favorable structure of the Ti-peroxo-complex is Ti–O–O–H and that the distances between both Ti which are 2.963 Å and 3.821 Å respectively are too long for an adsorption of H_2O_2 as Ti–O–O–Ti [28]. Lousada at al. [29] also confirm, by density functional theory, that this complex is the most stable.

Based on the surface OH density of TiO_2 P25 situated between 4.5 to 5.4 OH/nm^2 [30–33]. and the surface-OH density of TiO_2 Hombikat UV100 equal to 2.2 OH/nm^2 found by Du [33], our work shows that the more important the surface OH density the larger the number of H_2O_2 adsorbed per nm^2. The coverage rate of OH groups by H_2O_2 is around 50%. This suggests that two OH groups are necessary to adsorb one H_2O_2 molecule. Among the complex proposed in the literature, Ti–O–O–Ti will be the more adequate. However, the DFT studies [28,29], found that the distances between both Ti are too long for an adsorption of H_2O_2 as Ti–O–O–Ti. The most probable complex proposed in the literature Ti–O–O–H is not in agreement with the coverage rate observed in our condition. Moreover, considering the important stability of this complex it is difficult to consider that the yellow complex is TiOOH. Future researches are necessary to establish the nature of this complex.

3.4. Photocatalytic decomposition of H_2O_2

The disappearance of hydrogen peroxide at an initial concentration of about 5500 μmol/L under UV in presence of different TiO_2 samples and one ZnO sample are reported in Fig. 6 by plotting its evolution as a function of irradiation time. The direct photol-

Table 2
Adsorption constants (K_{dark}) in L/μmol and maximum amounts of H_2O_2 (Q_{max}) adsorbed in μmol/L and in molecules/nm^2 obtained from Langmuir model for different TiO_2 samples.

Oxides	P25	PC105	NA2	NA1	Hombikat	PC500	Rutile
K_{dark} (L/mol)	900	800	1110	1200	2300	2130	685
Q_{max} (μmol/g)	220	250	450	550	620	750	325
Q_{max} (molecules/nm^2)	2.7	1.5	1.2–1.3	1.3	1.3	1.3	1.9

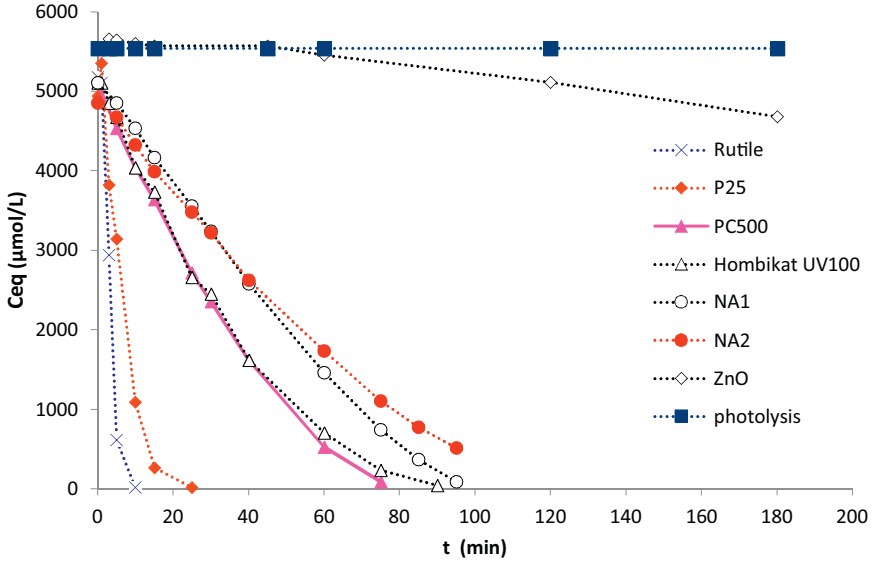

Fig. 6. Photocatalytic disappearance of the H_2O_2 concentration as a function of irradiation time, obtained on various TiO_2 and on one ZnO samples.

Table 3
Adsorption constants (K_{UV}) in L/µmol and disappearance rate constants of H_2O_2 (k) in µmol/L/min but also in molecule/s/nm^2 obtained from Langmuir–Hinshelwood model for different TiO_2 samples.

Oxides	P25	PC105	NA2	NA1	Hombikat	PC500	Rutile
k (µmol/L/min)	500	20	60	60	90	90	990
K_{UV} (L/µmol)	270	1020	440	440	330	450	230
k (molecule/s/nm^2)	0.15	0.0034	0.0044	0.0036	0.0044	0.0040	0.144

ysis of H_2O_2 at this wavelength was negligible indicating a true photocatalytic process.

From Fig. 6, we observed that rutile and TiO_2 P25 containing rutile structure have the highest disappearance rate compared to pure anatase.

For better understanding the photocatalytic activity of these different catalysts, for each catalyst the impact of H_2O_2 concentration on disappearance rate was evaluated. The initial rate of disappearance of H_2O_2 in presence of all photocatalysts is illustrated in Fig. 7a as a function of initial concentrations of H_2O_2 (C_e). Fig. 7b represents the initial rate of disappearance of H_2O_2 in presence of anatase structures only (PC105, AN1, AN2, PC500 and Hombikat catalysts). These curves show that, whatever the samples of TiO_2, the initial disappearance rates r_0 for H_2O_2 photodegradation increases rapidly as a function of the C_{eq} concentration, before reaching a plateau.

The curves in Fig. 7 seem compatible with the Langmuir–Hinshelwood model (Eq. (2)).

$$r_0 = \frac{kK_{UV}C_{eq}}{1 + K_{UV}C_{eq}} \quad (2)$$

where k is the rate constant of the reaction and K_{UV} is the equilibrium constant of adsorption of the substrate under the reaction. The linear transform enables one to determine the values of k and K_{UV} (Table 3)

First of all, it can be noted that adsorption constants determined under irradiation K_{UV} are different from the one obtained in the dark. All photocatalysts, except PC105 have a lower adsorption constant under irradiation. This behavior has already been observed in our laboratory [22], and by several other authors [23–25].

Several hypotheses have already been suggested to explain this phenomenon

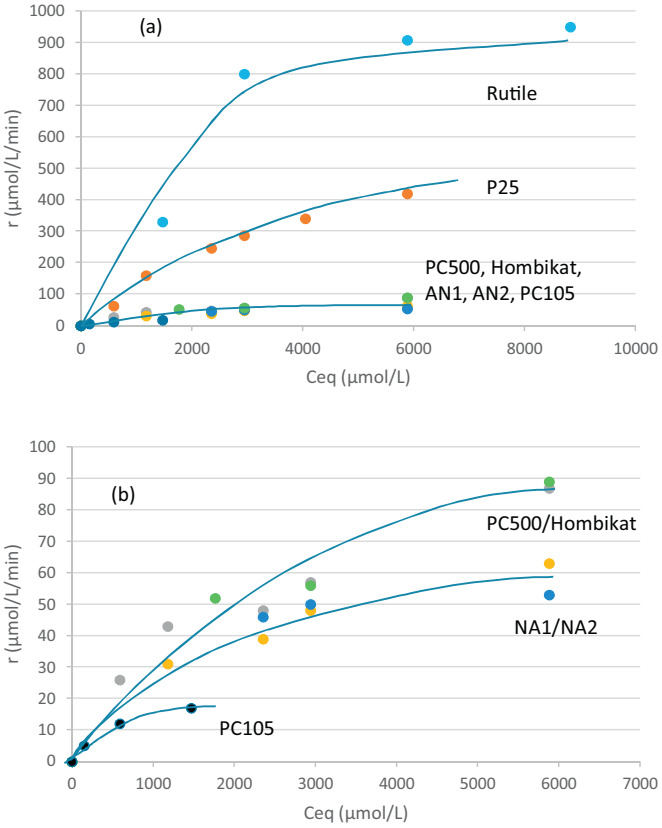

Fig. 7. Disappearance rate of H_2O_2 as a function of H_2O_2 concentration for all photocatalysts (a) and for only pure TiO_2 anatase (b).

- The reaction takes place on the surface but also near the surface [26,27].
- The active sites can be modified under UV-light considering the variation of the electronic properties of the TiO_2 surface under UV-irradiation.

($Ti^{4+} \rightarrow Ti^{3+}$; $O^{2-} \rightarrow O^{\bullet -}$) [34–40].

The surface area of the catalysts and the amount of H_2O_2 adsorbed play a role on the rate constants of H_2O_2 degradation

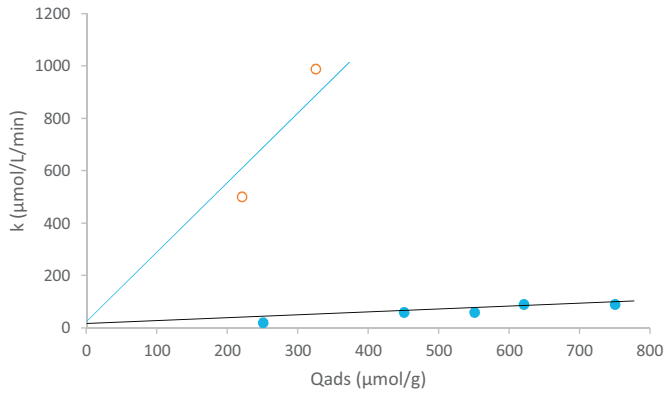

Fig. 8. Disappearance rate of H_2O_2 in presence of various TiO_2 samples as a function of the maximum concentration of adsorbed H_2O_2. Open circles correspond to TiO_2 containing rutile structure. Full circles correspond to pure anatase.

under UV irradiation. However, the most important parameter seems to be the presence of the rutile phase (Fig. 8).

Actually, H_2O_2 is rapidly degraded on rutile sample and on anatase mixed with rutile (TiO_2 P25) and much more slowly over the different anatase structures. The rate constant (k) expressed per molecules of H_2O_2 degraded per second and per unit of catalyst surface area is about 36 times higher for TiO_2 containing rutile structure ($k = 0.004+/-0.0005$ molecule/s/nm^2 for anatase structure and $0.145+/-0.005$ molecule/s/nm^2 for catalyst containing rutile).

The higher rate constants of H_2O_2 degradation in presence of TiO_2 containing rutile is in agreement with the results of Hirakawa et al. [2] and Zhang et al. [3]. These authors found that by addition of hydrogen peroxide the OH radical generation decrease on anatase but increase for rutile and rutile-contained TiO_2. Hirakawa et al. [2] also found that $O_2^{\bullet -}$ generation was smaller on rutile TiO_2. Whereas Hirakawa et al. suggest that OH radical were formed by reduction of H_2O_2, recently, two publications from the same team [3,42] conclude that H_2O_2 reacts with holes on both structures, anatase and rutile and that the increase of the OH radical with H_2O_2 for rutile TiO_2 may not be attributed to the reduction of H_2O_2 because of the higher formation of $O_2^{\bullet -}$ in presence of anatase TiO_2. However, to explain the increase of OH radical on rutile in presence of H_2O_2, they suggested that the formation of OH radical should be attributed to the oxidation of water assisted by the presence of H_2O_2. However, it is not clear how OH radicals can be formed by the oxidation of H_2O_2 by hole. Moreover, they also suggest the formation of Ti–O–O–Ti on rutile (not prove and reject by DFT [28]).

We can see that it is not very easy to explain the different rates of decomposition of H_2O_2 on anatase and rutile samples.

The higher decomposition of H_2O_2 on rutile is explained by considering (i) the difficulty to adsorb O_2 on rutile [41] and (ii) the values of the reduction potential of H_2O_2 and of O_2 with respect to the energy level of the conduction band of rutile versus that of anatase samples. In the case of anatase, the reduction of H_2O_2 is in competition with the reduction of O_2 whereas in the case of rutile, the reduction of H_2O_2 because of the difficulty of adsorption of O_2 and of the unfavorable energy level of its conduction band. Therefore, the oxidation of H_2O_2 should be favored on anatase (Reaction (R10)).

Our explanation is in agreement with the observations of Hirakawa et al. [2] and Zhang et al. [3] who showed (i) that in presence of H_2O_2, on rutile, OH radical generation was higher and $O_2^{\bullet -}$ generation was smaller because of the reaction of H_2O_2 with electrons (Reaction (R9)) and (ii) that the OH radical generation decrease on anatase TiO_2 because of the reaction of H_2O_2 with hole (Reaction (R10)) in competition with the reaction between H_2O and holes (Reaction (R5)).

$$H_2O_2 + e^- \rightarrow OH^{\bullet} + OH^- \quad \text{(R9)}$$

So, we propose that:

- On rutile, the decomposition of H_2O_2 is mainly due to its **reduction.**
- Whereas **on anatase**, H_2O_2 is mainly degraded by **oxidation**.

$$H_2O_2 + h^+ \rightarrow HO_2^{\bullet} + H^+ \quad \text{(R10)}$$

However, some point are not yet well explained, for example the observation of Kakuma et al. [42] showing that the reduction of O_2 on rutile did not decrease in the presence of H_2O_2. Is it due to the reaction of H_2O_2 with OH radical formed in high concentration? This hypothesis is not realistic because of the low rate of this reaction ($k = 2.7$ mol^{-1} L s^{-1}) [43]. However, this low rate could explain that OH radicals increase in presence of rutile but some of these hydroxyl radical are slowly transformed into $O_2^{\bullet -}$ explaining that this superoxide radical do not decrease in the presence of H_2O_2.

4. Conclusions

The adsorption capacity of H_2O_2 on TiO_2, modeled by the Langmuir model, depends on the structure and on the surface area of the photocatalysts. A surface density of about 1.2–1.5 was found for pure anatase whereas for pure rutile the surface density was 1.9 and equal to 2.7 for TiO_2 P25 containing rutile phase. The adsorption seems to be linked to the number of OH groups present on the surface of solids.

The rate constants of H_2O_2 disappearance in presence of the different TiO_2 samples, determined by using the Langmuir–Hinshelwood models, were correlated to the maximum amounts of H_2O_2 adsorbed on these materials and to the presence of rutile.

At similar amount of H_2O_2 adsorbed, the presence of rutile TiO_2 improves the decomposition of H_2O_2. More important the amount of rutile is more important the decomposition of H_2O_2 is.

The highest rate of H_2O_2 decomposition in presence of rutile was explained considering the energy levels of the conduction band of rutile and anatase. In the presence of anatase, the reduction of H_2O_2 is in competition with the reduction of O_2 whereas in presence of rutile samples, reduction of H_2O_2 is favored because of the difficulty of adsorption of O_2 and the unfavorable energy level of its conduction band. On rutile, H_2O_2 is mainly degraded by reduction whereas, on anatase, the main degradation of H_2O_2 occurs by oxidation. These hypotheses explain very well the active species generated on these both phases in presence of H_2O_2.

Taking into account the coverage rate and the important stability, in the dark, of the yellow complex formed between TiO_2 and H_2O_2, observed by UV–vis spectroscopy, Ti-μ-peroxide complex (TiOOH) proposed in the literature seems to be unlikely.

Acknowledgments

The authors gratefully acknowledge the financial support of the Algerian Ministry of Education and Research, and the University of Lyon, University Lyon 1 and the CNRS for receiving me.

References

[1] J. Yi, C. Bahrini, C. Schoemaecker, C. Fittschen, W. Choi, J. Phys. Chem. C 116 (2012) 10090–10097.
[2] T. Hirakawa, K. Yawata, Y. Nosaka, Appl. Catal. A: Gen. 325 (2007) 105–111.
[3] J. Zhang, Y. Nosaka, J. Phys. Chem. C 118 (2014) 10824–10832.

[4] P. Pichat, C. Guillard, L. Amalric, A.C. Renard, O. Plaidy, Sol. Energy Mater. Sol. Cells 38 (1995) 391–399.
[5] J.R. Harbour, J. Tromp, M.L. Hair, Can. J. Chem. 63 (1985) 204–208.
[6] C. Lousada, T. Brinck, M. Jonsson, Comput. Theor. Chem. 1070 (2015) 108–116.
[7] V. Augugliaro, E. Davi, L. Palmisano, M. Schiavello, A. Sclafani, Appl. Catal. 65 (1990) 101–116.
[8] B. Jenny, P. Pichat, Langmuir 7 (1991) 947–954.
[9] J. Schwitzgebel, J.G. Ekerdt, H. Gerisher, A. Heller, J. Phys. Chem. 99 (1995) 5633–5638.
[10] J. Thiebaud, F. Thevenet, C. Fittschen, J. Phys. Chem. C 114 (2010) 3082.
[11] Y. Nosaka, Y. Yamashita, H. Fukuyama, J. Phys. Chem. B 101 (1997) 5822–5827.
[12] G. Eisenberg, Ind. Eng. Chem. Anal. Ed. 15 (1943) 327–328.
[13] J. Rodier, B. Legube, N. Merlet, R. Brunet, 9ème ed., Dunod, 2009.
[14] M.V. Rao, K. Rajeshwar, V.R. Pai Verneker, J. Dubow, J. Phys. Chem. 84 (1980) 1987–1991.
[15] C. Kormann, D.W. Bahnemann, M. Hoffmann, Environ. Sci. Technol. 22 (1988) 798–806.
[16] A.H. Boonstra, C.A.H.A. Mutsaers, J. Phys. Chem. 79 (1975) 1940–1943.
[17] V. Maurino, C. Minero, G. Mariella, E. Pelizzetti, Chem. Commun. (2005) 2627–2629.
[18] H. Goto, Y. Hanada, T. Ohno, M. Matsumura, J. Catal. 225 (2004) 223–229.
[19] V. Diesen, M. Jonsson, J. Phys. Chem. C 118 (2014) 10083–10087.
[20] D. Tafalla, P. Salvador, J. Electroanal. Chem. 237 (1987) 225–236.
[21] T. Hirakawa, Y. Nosaka, Langmuir 18 (2002) 3247–3254.
[22] Y.K. Takahara, Y. Hanada, T. Ohno, S. Ushiroda, S. Ikeda, M. Matsumura, J. Appl. Electrochem. 35 (2005) 793–797.
[23] J. Su, G. Xiong, J. Zhou, W. Liu, D. Zhou, G. Wang, X. Wang, H. Guo, J. Catal. 288 (2012) 1–7.
[24] A.E. Regazzoni, P. Mandelbaum, M. Matsuyoshi, S. Schiller, S.A. Bilmes, M.A. Blesa, Langmuir 14 (1998) 868–874.
[25] X. Li, C. Chen, J. Zhao, Langmuir 17 (2001) 4118–4122.
[26] T. Ohno, Y. Masaki, S. Hirayama, M. Matsumura, J. Catal. 204 (2001) 163–168.
[27] C.C. Pavel, S. Park, A. Dreier, B. Tesche, W. Schmidt, Chem. Mater. 18 (2006) 3813–3820.
[28] W.F. Huang, P. Raghunath, M.C. Lin, J. Comput. Chem. 32 (2010) 1065–1081.
[29] C.M. Lousada, A.J. Johansson, T. Brinck, M. Jonsson, J. Phys. Chem. C 116 (2012) 9533–9543.
[30] H.P. Boehm, M.Z. Herrmann, Z. Anorg. Allg. Chem. (1967) 352.
[31] T. Rentschler, Farbe Lack 106 (2000) 62.
[32] R. Mueller, H.K. Kammler, K. Wegner, S.E. Pratsinis, Langmuir 1 (2003) 160–165.
[33] P. Du, J.A. Moulijn, G. Mul, J. Catal. 238 (2006) 342–352.
[34] M. El Madani, C. Guillard, N. Pérol, J.M. Chovelon, M. El Azzouzi, A. Zrinet, J.M. Herrmann, Appl. Catal. B: Environ. 65 (2006) 70–76.
[35] S. Parra, J. Oliveiro, C. Pulgarin, Appl. Catal. B: Environ. 36 (2002) 75–85.
[36] J. Cunningham, G.H. Al-Sayyed, S. Srijanarai, Aquatic and Surface Photochemistry, CRC Press, Boca Raton, FL, 2016, pp. 1994.
[37] A. Mells, S. Morris, J. Photochem. Photobiol. A: Chem. 71 (1993) 285–289.
[38] J. Cunningham, G.H. Al-Sayyed, J. Chem. Soc. Faraday Trans. 86 (1990) 3935–3941.
[39] J. Cunningham, P. Sedlak, in: D.F. Ollis, H. Al-Ekabi (Eds.), Photocatalytic Purification and Treatment of Water and Air, Elsevier, Amsterdam, 2016, p. 1993.
[40] Y. Xu, C.H. Langford, J. Photochem. Photobiol. A: Chem. 133 (2000) 67–71.
[41] Q. Sun, Y. Xu, J. Phys. Chem. C 114 (2010) 18911–18918.
[42] Y. Kakuma, A.Y. Nosaka, Y. Nosaka, Phys. Chem. Chem. Phys. 17 (2015) 18691.
[43] H. Christensen, K. Sehested, H. Corfitzen, J. Phys. Chem. 86 (1982) 1588.